# Enlargement or Reduction of Digital Images with Minimum Loss of Information

Michael Unser, *Senior Member, IEEE*, Akram Aldroubi, and Murray Eden, *Life Fellow, IEEE*

*Abstract*—**The purpose of this paper is to derive optimal spline algorithms for the enlargement or reduction of digital images by arbitrary (noninteger) scaling factors. In our formulation, the original and rescaled signals are each represented by an interpolating polynomial spline of degree $n$ with step size one and $\Delta$, respectively. The change of scale is achieved by determining the spline with step size $\Delta$ that provides the closest approximation of the original signal in the $L_2$-norm. We show that this approximation can be computed in three steps: i) a digital prefilter that provides the $B$-spline coefficients of the input signal, ii) a resampling using an expansion formula with a modified sampling kernel that depends explicitly on $\Delta$, and iii) a digital postfilter that maps the result back into the signal domain. We provide explicit formulas for $n = 0$, 1, and 3 and propose solutions for the efficient implementation of these algorithms. We consider image processing examples and show that the present method compares favorably with standard interpolation techniques. Finally, we discuss some properties of this approach and its connection with the classical technique of bandlimiting a signal, which provides the asymptotic limit of our algorithm as the order of the spline tends to infinity.**

## I. Introduction

RESAMPLING is used extensively in picture processing to magnify or reduce images and to correct for spatial distortions. Standard approaches fit the original data with a continuous model (image interpolation) and then resample this two-dimensional function on a new sampling grid [1], [2]. In the case of nearest neighbor interpolation, the underlying image model is a polynomial spline of order zero (piecewise constant). This is extremely simple to implement but tends to produce images with a blocky appearance. More satisfactory results can be obtained with bilinear interpolation, which uses an implicit first order spline model, or by using small-kernel cubic convolution techniques (piecewise cubic model) [2]–[5]. Bicubic spline interpolation [6], and higher order splines in general [7], yield even smoother recontructions; fast algorithms using digital filters are also available [8].

These approaches are reasonably simple to implement, but they tend to produce sub-optimal results because they are not designed to minimize information loss. This is especially true for image reduction. Such problems can be avoided if one uses some form of lowpass filtering prior to resampling, a principle commonly used for sampling rate conversion in multirate signal processing [9]–[11]. Such a prefiltering step is also required for decimation based on the principle of least squares spline approximation [12]–[14]. Fig. 1 provides a comparison between the simplest form of this procedure (zero order spline approximation) and straightforward resampling. Unfortunately, such filtering-decimation techniques are restricted to situations in which the reduction factor $m$ is an integer.[1] These limitations notwithstanding, we believe that comparisons such as the one afforded by Fig. 1 provide a convincing illustration of the fact that interpolation is sub-optimal when used for image reduction. Interpolation may also introduce distortion in the case of nonintegral signal magnification. This effect is especially noticeable for zero order interpolation (c.f. Fig. 2). Fortunately, it tends to disappear when higher order splines are applied.

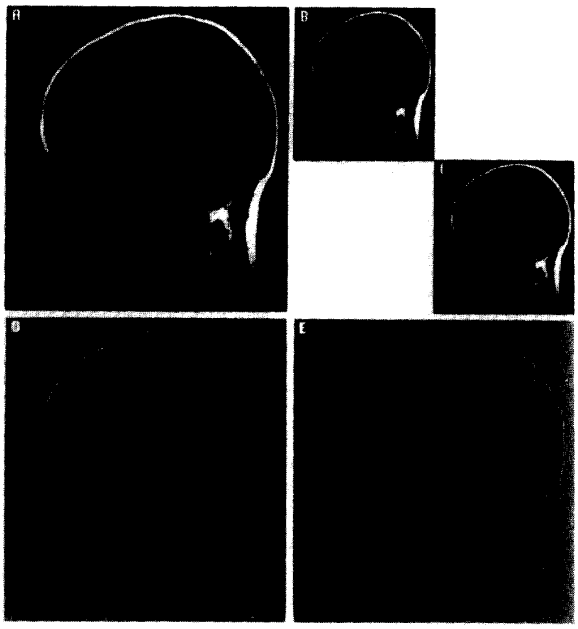


Fig. 1. Resampling versus least squares approximation for image reduction by a factor of two using a zero order interpolation model (piecewise constant): (a) Original MRI image; (b) reduction by simple resampling (interpolation); (c) reduction by averaging over a 2 × 2 neighborhood (least squares approximation); (d) approximation error for (b) (SNR=24.74 dB); (e) approximation error for (c) (SNR=29.50 dB).

Manuscript received June 12, 1992; revised November 17, 1993. The associate editor coordinating the review of this paper and approving it for publication was Prof. Avideh Zakhor.

The authors are with the Biomedical Engineering and Instrumentation Program, National Center for Research Resources, National Institutes of Health, Bethesda, MD 20892-5766 USA.

IEEE Log Number 9408199.

[1] The use of these techniques can eventually be extended for rational factor $m_1/m_2$ by first interpolating the input signal. In that case, however, they lose most of their computational appeal.

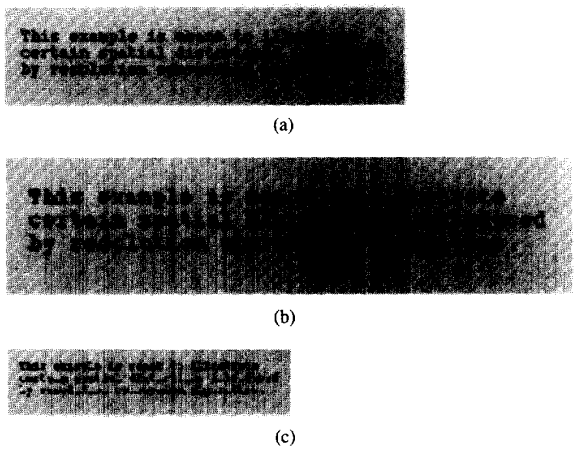

(a) (b) (c)

Fig. 2. Examples of artifacts induced by zero-order (or nearest neighbor) interpolation in the case of a nonintegral scaling factor: (a) Original text image; (b) magnification by a factor of $\sqrt{2}$; (c) reduction by a factor of $\sqrt{2}$. Note that the distortion of the letters in (b) is nonuniform. The text in (c) is degraded to a point that it is unreadable.

In this paper, we address these problems directly and develop least squares polynomial spline resampling algorithms for an arbitrary step size $\Delta$. The basis for this new formulation is our recent extension of Hummel's sampling theory for polynomial splines [12], [15]. The main point of this work will be to establish that optimal signal resampling by splines can be obtained by the combination of digital filters and an interpolation in the conventional sense with a modified sampling function $\xi_\Delta^n(x)$ that depends on the sampling step $\Delta$. This procedure is easy to implement because the sampling kernel $\xi_\Delta^n(x)$ is compactly supported. We will also show that the present method provides a generalization of a number of earlier approaches. Moreover, it converges to the optimal procedure for bandlimited signals dictated by Shannon's sampling theorem as the order of the spline goes to infinity.

The presentation is organized as follows. In Section II, we review some fundamental properties of polynomial splines and give the main results of their sampling theory based on the principle of minimum error approximation. In Section III, we derive an optimal scale conversion algorithm for splines of any order $n$ and discuss its implementation with an emphasis on its digital filtering components. In Section IV, we obtain explicit formulas for the sampling function $\xi_\Delta^n(x)$ for piecewise constant ($n = 0$), linear ($n = 1$), and cubic splines ($n = 3$). Finally, in Section V, we present some experimental results, both qualitative and quantitative, and provide a comparison with conventional techniques.

### A. Notation and Operators

$L_2$ is the vector space of measurable, square-integrable functions $g(x)$, $x \in R$. $L_2$ is a Hilbert space whose metric $\|\cdot\|$ (the $L_2$-norm) is derived from the inner product

$$\langle g, h\rangle = \langle g(x), h(x)\rangle = \int_{-\infty}^{+\infty} g(x)h(x)dx$$

$$\|g\| = \sqrt{\langle g, g\rangle} = \left(\int_{-\infty}^{+\infty} |g(x)|^2 dx\right)^{\frac{1}{2}}.$$

The central $B$-spline of order $n$ is denoted by $\beta^n(x)$; this function, a piecewise polynomial of degree $n$, is generated by repeated convolution of a $B$-spline of order 0

$$\beta^n(x) = \beta^0 * \beta^{n-1}(x) \tag{1}$$

with

$$\beta^0(x) = \begin{cases} 1, & x \in \left[-\frac{1}{2}, \frac{1}{2}\right) \\ 0, & \text{otherwise.} \end{cases} \tag{2}$$

The space of square summable sequences (or discrete signals) $a(k)$, $k \in Z$ is $l_2$. The convolution of two sequences $a \in l_2$ and $b \in l_2$ is denoted by $b^* a(k)$. The sequence $b$ may be viewed as a discrete convolution operator (or digital filter) applied to $a$; it is entirely characterized by its $z$-transform (or transfer function) $B(z)$. If $B(z)$ has no zeros on the unit circle, then the inverse operator $(b)^{-1}$ exists and is uniquely defined

$$(b)^{-1}(k) \overset{z}{\longleftrightarrow} 1/B(z). \tag{3}$$

A special notation is used for the discrete $B$-spline of order $n$, which is obtained by sampling $\beta^n(x)$ at integral values

$$b^n(k) = \beta^n(x)|_{x=k} \overset{z}{\longleftrightarrow} B_1^n(z). \tag{4}$$

The sequence $(b^n)^{-1}(k)$ represents the impulse response of the direct $B$-spline filter of order $n$ [8]. This filter has been shown to be stable for all values of $n$ [7].

## II. Polynomial Splines

In this section, we review some properties of polynomial splines crucial for the derivation of the scale conversion algorithm in Section III. A more detailed treatment of various aspects of spline interpolation, spline representation, and spline approximations can be found in [7], [8], [14], and [15], respectively.

### A. Polynomial Spline Function Spaces

In our formulation, signals are represented by polynomial splines. These functions are piecewise polynomials of degree $n$ with the additional smoothness constraint that the polynomial segments are connected in a way that insures the continuity of the function and its derivatives up to order $n-1$. At the initial scale ($\Delta = 1$), there is exactly one knot per sample value (or pixel) and the signal is represented by a spline that provides an exact interpolation. The corresponding spline function space $S_1^n$ can be defined as follows [16], [17]:

$$S_1^n = \left\{ s^n(x) = \sum_{k=-\infty}^{+\infty} c(k)\beta^n(x-k) \colon c \in l_2 \right\} \tag{5}$$

where $\beta^n(x)$ is the central $B$-spline function of order $n$ defined by (1). The fundamental characteristic of the $B$-spline basis functions is their compact support, the property that makes them useful in a variety of applications [18], [19].

It is also possible to construct alternative sets of shift invariant basis functions by taking linear combinations of $B$-splines. This result can be stated as follows (cf. [14], Appendix A):

*Proposition 1 (Equivalent Basis Functions):* The set of functions $\{\varphi^n(x-k), k \in Z\}$ with

$$\varphi^n(x) = \sum_{k=-\infty}^{+\infty} p(k)\beta^n(x-k) \tag{6}$$

is a basis of $S_1^n$ provided that $p$ is an invertible convolution operator from $l_2$ into itself.

Hence, we have the generalized spline representation

$$s^n(x) = \sum_{k=-\infty}^{+\infty} d(k)\varphi^n(x-k) \tag{7}$$

which is entirely specified by the sequence of coefficients $d(k) \in l_2$. Two special cases that are especially relevant (the cardinal and dual representations) are discussed below.

### B. Cardinal Spline Interpolation

In order to fit the model to the data points, one first needs to determine the $B$-spline coefficients of a $s^n(x)$ that interpolates the digital signal $\{s(k)\}_{k\in Z}$. The simplest approach is to use a digital filter [8]

$$c(k) = (b^n)^{-1} * s(k) \tag{8}$$

where $(b^n)^{-1}$ denotes the convolution inverse of the discrete $B$-spline kernel defined by (4).

By further substituting (8) in (5), we obtain the equivalent cardinal representation of the interpolating spline $s^n(x)$, in which the expansion coefficients are precisely the sample values $s(k)$:

$$\begin{aligned} s^n(x) &= \sum_{k=-\infty}^{+\infty} (b^n)^{-1} * s(k)\beta^n(x-k) \\ &= \sum_{k=-\infty}^{+\infty} s(k)\ \eta^n(x-k). \end{aligned} \tag{9}$$

$\eta^n(x)$ is the *cardinal (or fundamental)* spline of order $n$, which is given by (6) with $p_c = (b^n)^{-1}$. It is the spline equivalent of the classical sinc interpolation kernel [7].

Having made these definitions, we can interpret the process of $B$-spline interpolation (cf. (8)) as a coordinate change from cardinal to $B$-spline representation.

### C. Polynomial Spline Sampling Theory

We now consider the problem of the approximation of a function $s(x) \in L_2$ by splines with a step size $\Delta$. The corresponding space $S_\Delta^n$ is defined by simple rescaling; i.e., $h(x) \in S_\Delta^n \Leftrightarrow h(\Delta x) \in S_1^n$. The optimal approximation in the $L_2$-norm is obtained by projecting $s$ on $S_\Delta^n$. This procedure is accomplished as follows (c.f [14], [15]):

*Theorem 2 (General Sampling Theorem):* The orthogonal projection of a function $s \in L_2$ on $S_\Delta^n$ can be evaluted as

$$s_\Delta^n(x) = \sum_{k=-\infty}^{+\infty} \frac{1}{\Delta}\langle s(x), \overset{\circ}{\varphi}{}^n(x/\Delta - k)\rangle \varphi^n(x/\Delta - k) \tag{10}$$

where $\varphi^n$ is defined by (6) (with $p$ symmetrical and invertible), and where

$$\overset{\circ}{\varphi}{}^n(x) = \sum_{k=-\infty}^{+\infty} (p * b^{2n+1})^{-1}(k)\beta^n(x-k) \tag{11}$$

is the corresponding biorthogonal sampling function.

Similar to Hummel [12], we can interpret the sampling function $\overset{\circ}{\varphi}{}^n$ as an optimal prefilter that is applied to $s$ prior to sampling, and $\varphi^n$ as a reconstruction filter. Theorem 2 may therefore be viewed as an extension of the standard signal processing approach to discretization dictated by Shannon's sampling theorem [20]. In fact, we have shown that the functions $\overset{\circ}{\eta}{}^n$ and $\eta^n$ (cardinal representation) both converge to $\mathrm{sinc}(x)$ as the order of the spline tends to infinity [7], [15].

Note that the simplest expression for the sampling function $\overset{\circ}{\varphi}{}^n$ in (11) occurs for $p_d = (b^{2n+1})^{-1}$, in which case it is precisely a $B$-spline of order $n$. The corresponding generating function in (6) is the *dual* spline: $\overset{\circ}{\beta}{}^n(x)$. In this representation, the calculation of the inner products in (10) is especially simple since the corresponding sampling function is compactly supported. This property turns out to be crucial for the implementation of the scale conversion algorithms considered in Sections III and IV.

### D. Extension in Higher Dimensions

Although all our results will be presented for the one-dimensional case, they are directly applicable to higher dimensions through the use of tensor product splines [19]. The corresponding basis functions are simply obtained from the product of one-dimensional functions of the individual index variables. Practically, this means that the corresponding interpolation and approximation algorithms are separable and can be implemented by successive one-dimensional processing along the rows and columns of an image. This observation applies for the implementation of digital filters as well as for the resampling of two-dimensional expansion formulas.

We now provide a short proof of this latter result that is not as well known in signal processing. Consider the problem of resampling the general separable 2D expansion

$$g(x,y) = \sum_{k=-\infty}^{+\infty}\sum_{l=-\infty}^{+\infty} d(k,l)\varphi(x-k)\varphi(y-l) \tag{12}$$

on a uniform sampling grid with horizontal and vertical sampling step $\Delta_x$, and $\Delta_y$, respectively. The key observation is that the sampled version of this expansion can be rewritten as

$$\begin{aligned} g(i\Delta_x, j\Delta_y) &= \sum_{k=-\infty}^{+\infty}\sum_{l=-\infty}^{+\infty} d(k,l)\varphi(i\Delta_x - k)\varphi(j\Delta_y - l) \\ &= \sum_{l=-\infty}^{+\infty} g_x(i.l)\varphi(j\Delta_y - l) \end{aligned} \tag{13}$$

where

$$g_x(i,l) = \sum_{k=-\infty}^{+\infty} d(k,l)\varphi(i\Delta_x - k). \tag{14}$$

Hence, the calculation can be performed in two successive passes using one-dimensional summations only. The first is a resampling along the $x$-direction according to (14), while the second is a resampling in the $y$-direction using the modified coefficients $g_x(i,l)$. Such a separable implementation can result in a substantial saving in computations, especially when the support of the sampling function $\varphi$ is large.

## III. Optimal Scale Conversion

The most direct approach to signal magnification (or reduction) by a factor $\Delta$ is to use the $B$-spline representation (5) and to resample this function at multiples of $\Delta$. This approach is perfectly practical because the $B$-splines have compact support; consequently, there is only a finite number of coefficients that contribute to the value of the function for a given ordinate $x$. The expansion formula is easy to evaluate numerically. This approach is the one most frequently used in image processing applications; in particular, for $n = 0$ (nearest neighbor interpolation) and $n = 1$ (bilinear interpolation).

As far as the approximation error is concerned, this procedure is suboptimal. In the case of a reduction, the situation is analogous to sampling a signal that has not been previously bandlimited, a process that may induce aliasing errors. Next, we derive a general least squares approximation technique to avoid these types of artifacts.

### A. Scale Conversion

By convention, we assume that the initial sampling step is one. Our input signal is described by its $B$-spline representation $s_1^n(x) \in S_1^n$

$$s_1^n(x) = \sum_{k=-\infty}^{+\infty} c_1(k)\beta^n(x-k) \tag{15}$$

The relation between the signal values and the $B$-spline coefficients is one-to-one; in other words, there is exactly one $B$-spline coefficient per initial grid point.

The step size on the resampled version of our signal is $\Delta$. The corresponding new signal approximation is represented by a polynomial spline $s_\Delta^n(x) \in S_\Delta^n$:

$$s_\Delta^n(x) = \sum_{k=-\infty}^{+\infty} c_\Delta(k)\beta^n(x/\Delta - k) \tag{16}$$

with a knot spacing $\Delta$. Note that a step size $\Delta < 1$ corresponds to a signal magnification (i.e., there are more samples within a given signal segment) whereas a step size $\Delta > 1$ results in a size reduction (data compression).

The scale conversion problem can now be formulated as follows: *Given a function $s_1^n(x) \in S_1^n$, find its minimum error approximation $s_\Delta^n(x)$ in the space $S_\Delta^n$.*

The solution then follows from the application of Theorem 2. To simplify this computation, we use the equivalent dual representation of $s_\Delta^n(x)$

$$s_\Delta^n(x) = \sum_{k=-\infty}^{+\infty} d_\Delta(k)\mathring{\beta}^n(x/\Delta - k) \tag{17}$$

where the dual spline $\mathring{\beta}(x)$ is a polynomial spline with $B$-spline coefficients $p_d = (b^{2n+1})^{-1}$. From Theorem 2, we get the expression for the optimum expansion coefficients in (17)

$$d_\Delta(k) = \frac{1}{\Delta}\langle s_1^n(x),\ \beta^n(x/\Delta - k)\rangle.$$

Replacing $g_1^n(x)$ by its $B$-spline expansion (15), we find that

$$d_\Delta(k) = \frac{1}{\Delta}\sum_{l=-\infty}^{+\infty} c_1(l)\langle \beta^n(x-l), \beta_\Delta^n(x-k\Delta)\rangle$$

where $\beta_\Delta^n(x) := \beta^n(x/\Delta)$. Using the symmetry of the $B$-splines, we then rewrite this expression in the more convenient form

$$d_\Delta(k) = \sum_{l=-\infty}^{+\infty} c_1(l)\xi_\Delta^n(k\Delta - l) \tag{18}$$

where the sampling function $\xi_\Delta^n$ is defined as

$$\xi_\Delta^n(x) = \frac{1}{\Delta}(\beta^n * \beta_\Delta^n)(x). \tag{19}$$

Since both functions are compactly supported, the kernel $\xi_\Delta^n$ in (19) is as well. Hence, there is only a finite number of coefficients in (18) that contribute to the value of $d_\Delta(k)$ for a fixed index $k$. This sum can therefore be evaluated exactly provided that one has an explicit formula for the sampling function $\xi_\Delta^n(x)$. Such formulas are given in Section IV.

We also note that the integral of the function $\xi_\Delta^n$ is normalized to one. This result can be established simply by evaluating the value of the Fourier transform of (19) at the origin.

### B. Implementation

In practice, the signals on both sampling grids are represented by their respective sample values $s_1(k)$ and $s_\Delta(k)$. Hence, we have the equivalent cardinal spline representations

$$s_1^n(k) = \sum_{k=-\infty}^{+\infty} s_1(k)\eta^n(x-k) \tag{20}$$

$$s_\Delta^n(x) = \sum_{k=-\infty}^{+\infty} s_\Delta(k)\eta^n(x/\Delta - k). \tag{21}$$

The scale conversion algorithm should take the values $s_1(k)$ as input and return the samples $g_\Delta(k)$ of the least squares spline approximation in $S_\Delta^n$. This can be achieved by combining the procedure described above (cf. (18)) with the appropriate changes of coordinate system. The full algorithm represented in Fig. 3 can be summarized as follows:

i) Determine the $B$-spline coefficients in (16). This operation is equivalent to processing the data with the prefilter $p = (b^n)^{-1}$ (c.f. Section II-B).
ii) Expand linearly and sample according to (18).

TABLE I
TRANSFER FUNCTIONS OF THE FILTERS FOR THE LEAST SQUARES SPLINE SCALE CONVERSION ALGORITHM FOR $n = 0$, 1, AND 3

| $n$ | P(z) | Q(z) |
|---|---|---|
| 0 | 1 | 1 |
| 1 | 1 | $\frac{6}{z+4+z^{-1}}$ |
| 3 | $\frac{6}{z+4+z^{-1}}$ | $\frac{840(z+4+z^{-1})}{2416+1191[z+z^{-1}]+120[z^2+z^{-2}]+[z^3+z^{-3}]}$ |

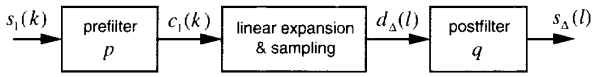


Fig. 3. General block diagram of the optimal scale convertion algorithm.

iii) Convert from dual to cardinal spline representation. This is implemented by post-filtering

$$s_\Delta(k) = q * d_\Delta(k); \quad q = \left(b^{2n+1}\right)^{-1} * b^n. \tag{22}$$

The $z$-transforms of the corresponding pre- and post-filters for $n = 0$, 1 and 3 are given in Table I. No filters are required for piecewise constant approximation ($n = 0$). In the case of a piecewise linear model ($n = 1$), there is only the postfilter. Interestingly, it is identical to the prefilter for the cubic spline approximation ($n = 3$).

## IV. EVALUATION OF THE SAMPLING KERNELS

The last practical aspect that needs to be dealt with is the explicit evaluation of the modified sampling kernel in (18) defined by (19). Here, we present the results of these calculations for $n = 0$ and 1 and provide a Gaussian approximation formula for higher order splines. Finally, we consider the limiting case of bandlimited functions and describe an FFT-based algorithm for that particular case.

### A. Piecewise Constant

The expression of a $B$-spline of order zero is given by (2). The explicit evaluation of (19) for $n = 0$ yields

$$\xi_\Delta^0(x) = \begin{cases} b, & 0 \le |x| < a_1 \\ b - \frac{b(|x|-a_1)}{a_2-a_1}, & a_1 \le |x| < a_2 \\ 0, & a_2 \le |x| \end{cases} \tag{23}$$

where the constants $b, a_1$, and $a_2$ are defined as follows:

$$\begin{cases} b = \min\{1, \Delta\}/\Delta \\ a_1 = \min\{1, \Delta\}/2 \\ a_2 = (1+\Delta)/2. \end{cases} \tag{24}$$

The corresponding sampling function is piecewise linear. An example for $\Delta = 3/2$ is represented in Fig. 4. Note that for $\Delta = 1, \xi_\Delta^0(x)$ is the $B$-spline of order 1.

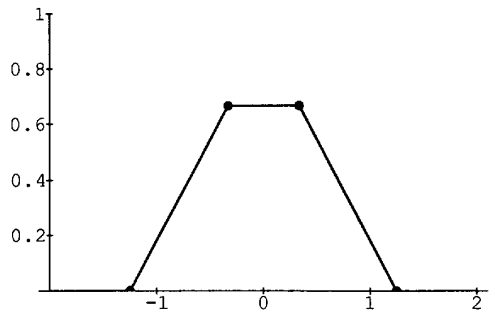


Fig. 4. Example of trapezoidal sampling function for a zero order spline model ($\Delta = 3/2$).

### B. Piecewise Linear

The $B$-spline of order 1 is the tent function described by the formula

$$\beta^1(x) = \begin{cases} 1 - |x|, & |x| \le 1 \\ 0, & |x| \ge 1 \end{cases} \tag{25}$$

In order to compute $\xi_\Delta^1(x)$, we chose to take the first derivatives of $\beta^1(x)$ and $\beta_\Delta^1(x)$, to evaluate their cross-correlation function, which is piecewise linear, and finally to integrate this function twice to get the desired result. The result of this rather lengthy computation is a symmetrical cubic spline function with unequally spaced knots $\{-a_4, -a_3, -a_2, -a_1, a_0, a_1, a_2, a_3, a_4\}$. The values of these points are given by

$$\begin{cases} a_0 = 0 \\ a_1 = \min\{a, b-a\} \\ a_2 = \max\{a, b-a\} \\ a_3 = b \\ a_4 = a + b \end{cases} \tag{26}$$

where the constants $a$ and $b$ are defined as follows:

$$\begin{cases} a = \min\{1, \Delta\} \\ b = \max\{1, \Delta\}. \end{cases} \tag{27}$$

For each segment $i, \xi_\Delta^1(x)$ is a cubic polynomial. This function can therefore be represented by the formula

$$\xi_\Delta^1(x) = \begin{cases} b_{i0} + b_{i1}|x| + b_{i2}x^2 + b_{i3}|x|^3, & |x| \in [a_{i-1}, a_i) \\ 0, \text{otherwise} \end{cases} \tag{28}$$

where the polynomial coefficients for $i = 1, \ldots, 4$ are given in Table II. For $\Delta = 1$, some of the knot points merge and one can verify that $\xi_1^1(x)$ is precisely a cubic $B$-spline. An example of the sampling function with $\Delta = 3/4$ is shown in Fig. 5. To emphasize the Gaussian-like shape of this kernel, we have superimposed with a dashed line the Gaussian approximation given by (30) below.

### C. Cubic and Higher Order Splines

The cubic $B$-spline ($n = 3$) is given by

$$\beta^3(x) = \begin{cases} 2/3 - x^2 + |x|^3/2, & 0 \le |x| < 1 \\ (2-|x|)^3/6, & 1 \le |x| < 2 \\ 0, & 2 \le |x| \end{cases} \tag{29}$$

TABLE II
POLYNOMIAL COEFFICIENTS FOR THE SAMPLING FUNCTIONS

| Interval | $b_0$ | $b_1$ | $b_2$ | $b_3$ |
|---|---|---|---|---|
| $0 \le \lvert x\rvert \le a_1$ | $\frac{-a(a-3b)}{3b\Delta}$ | 0 | $\frac{-1}{b\Delta}$ | $\frac{1}{3ab\Delta}$ |
| $a_1 \le \lvert x\rvert < a_2$ | | | | |
| (i) $a \le (b-a)$ | $\frac{a}{\Delta}$ | $\frac{-a}{b\Delta}$ | 0 | 0 |
| (ii) $a > (b-a)$ | $\frac{-(a+b)(a^2-4ab+b^2)}{6ab\Delta}$ | $\frac{(a-b)^2}{2ab\Delta}$ | $\frac{-(a+b)}{2ab\Delta}$ | $\frac{1}{2ab\Delta}$ |
| $a_2 \le \lvert x\rvert < a_3$ | $\frac{a^3+3a^2b+3ab^2-b^3}{6ab\Delta}$ | $\frac{-a^2-2ab+b^2}{2ab\Delta}$ | $\frac{(a-b)}{2ab\Delta}$ | $\frac{1}{6ab\Delta}$ |
| $a_3 \le \lvert x\rvert < a_4$ | $\frac{(a+b)^3}{6ab\Delta}$ | $\frac{-(a+b)^2}{2ab\Delta}$ | $\frac{(a+b)}{2ab\Delta}$ | $\frac{-1}{6ab\Delta}$ |
| $a_4 \le \lvert x\rvert$ | 0 | 0 | 0 | 0 |

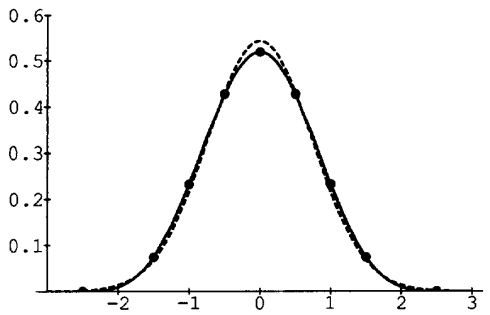


Fig. 5. Example of a modified sampling function (solid line) for a first order spline model ($\Delta = 3/2$). This function is a cubic spline with knot points at the positions marked by the small circles. The Gaussian approximation given by (34) is superimposed with a dashed line (relative mean square error = 0.145%).

Evaluating $\xi_\Delta^n(x)$ for this particular case as well as for higher order splines becomes more and more cumbersome. Instead, we have chosen to derive a Gaussian approximation. This approach is justified by the fact that $\xi_\Delta^n(x)$ can be expressed as a convolution product of multiple rectangular pulses. As $n$ increases, this function converges to a Gaussian, as a consequence of the central limit Theorem (c.f. [21]). To determine the parameters of this limiting form, we use the property that the global variance of a convolution product is equal to the sum of the variances of its individual components. Hence, we obtain the following approximation

$$\xi_\Delta^n(x) \cong \begin{cases} \frac{1}{\sqrt{2\pi}\sigma_n} \exp\left\{\frac{-x^2}{2\sigma_n^2}\right\}, & |x| < \frac{n+1}{2}(1+\Delta) \\ 0, & \text{otherwise} \end{cases} \quad (30)$$

with standard deviation

$$\sigma_n = \sqrt{\frac{n+1}{12}(1+\Delta^2)}. \quad (31)$$

Note that this formula is truncated to accommodate for the fact that the function $\xi_\Delta^n(x)$ is compactly supported. The Gaussian in (30) is such that it has the same integrated area ($\int \xi_\Delta^n(x)dx = 1$) and variance ($\sigma_n^2 = \int x^2 \xi_\Delta^n(x)dx$) as the true sampling kernel $\xi_\Delta^n(x)$. The approximate sampling function for the cubic spline is obtained by setting $n = 3$ in (31) and (30). The quality of this approximation should be sufficient for most practical purposes. For example, we found that the relative mean square error for $n = 3$ and $\Delta = 3/4$ was less than 0.04% (this computation was performed in the Fourier domain). Note that for $\Delta = 1, \xi_1^3(x)$ is precisely the $B$-spline of order 7.

### D. The Bandlimited Case

The cardinal generating function for the bandlimited representation of a signal is

$$\eta^\infty(x) = \text{sinc}(x) \quad (32)$$

By using the fact that the Fourier transform of $\text{sinc}(x)$ is $\text{rect}(f)$, it is not difficult to show that the corresponding modified sampling kernel is

$$\xi_\Delta(x) = \frac{1}{\Delta}\eta_\Delta^\infty * \eta^\infty(x) = \begin{cases} \text{sinc}(x), & \Delta \le 1 \\ \frac{1}{\Delta}\text{sinc}(x/\Delta), & \Delta > 1. \end{cases} \quad (33)$$

Note that no pre- and postfilters are necessary since the expansion coefficients are precisely the samples of the underlying continuous function (cardinal representation). In principle, the samples of the rescaled signal can be evaluated directly through the expansion formula (18), although the slow decay of the sinc function requires the evaluation of a relatively large number of terms.

This procedure can be implemented much more efficiently in the Fourier domain provided that the scaling factor is a rational number $\Delta = m_1/m_2$, where $m_1$ and $m_2$ are the sizes of the input and output signal arrays, respectively [22], [23]. For this purpose, we use the property that a bandlimited signal is entirely represented by the discrete Fourier transform of its sampled values. The first step of the algorithm is to perform an $m_1$-point FFT. These values are then copied into an $m_2$-point complex array using zero padding in the case of a signal expansion, or by disregarding the values with an index larger than $m_2$ otherwise. Note that this latter operation corresponds to the antialiasing low-pass filtering step. An additional multiplication by $(1/\Delta)$ is also required for signal reduction (c.f. (33)). The rescaled output signal is then simply obtained by performing an $m_2$-points inverse FFT.

## V. EXPERIMENTAL RESULTS

### A. Implementation

The spline scaling algorithms were implemented on a personal computer. We used a separable algorithm in which the rows and columns of an image are processed in succession. All 1–D computations were performed in floating point and the digital filters were implemented recursively, as described in [24]. The organization of the program more or less replicated the block diagram in Fig. 3. To save memory space, all digital images, as well as the intermediate results of computations, were truncated and stored in integer format with two bytes per pixel; appropriate scaling factors were used to minimize truncation errors.

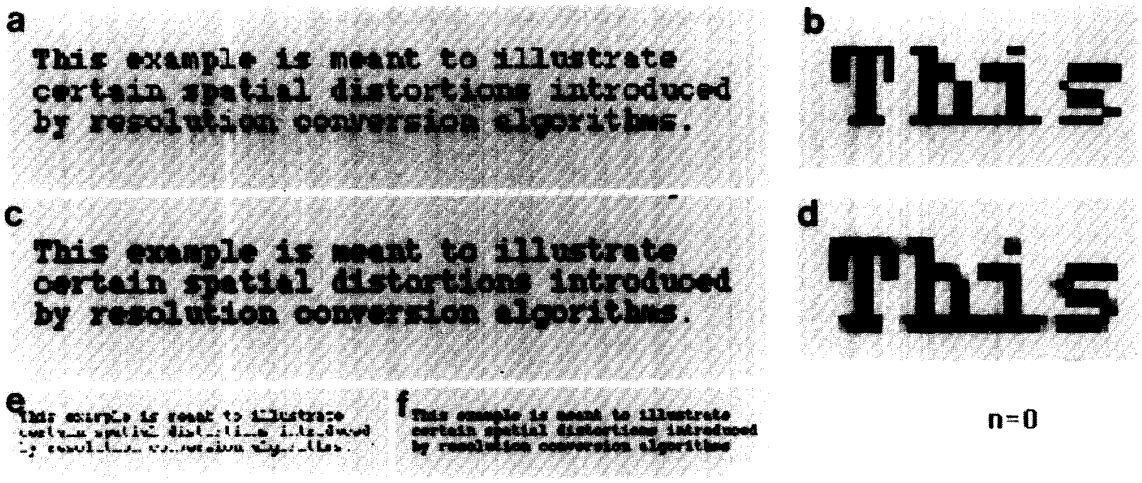


Fig. 6. Examples of image magnification and reduction using a zeroth-order model: (a) ISC0 with $\Delta = 1/\sqrt{2}$; (b) enlarged detail of (a); (c) LSSC0 with $\Delta = 1/\sqrt{2}$; (d) enlarged detail of (c); (e) ISC0 with $\Delta = \sqrt{2}$; (f) LSSC0 with $\Delta = \sqrt{2}$.

The conventional interpolation approach was implemented by using the same technique and simply replacing the function $\xi_{\Delta}^{n}(x)$ by $\beta^{n}(x)$. The use of a postfilter was not necessary in this case.

For the implementation of the cubic spline approximation algorithm, we used the approximate Gaussian form (30) of the sampling kernel. We also modified the postfilter slightly to insure that the algorithm provides a perfect signal restitution for $\Delta = 1$. Specifically, we substituted the kernel $(b^{2n+1})$ in (22) by the sampled version of the Gaussian approximation of $\xi_{1}^{n}(x)$ obtained from (30). The resulting transfer function of the cubic spline postfilter that was used for our experiments is shown in (34), which appears at the bottom of this page. All algorithms were applied to some test images with $\Delta = 1$. In all cases, the reconstructed images were identical to the input, a reasonable indication that the effect of truncation and roundoff errors was not significant.

In the sequel, the different techniques are referred to by the following acronyms: interpolative scale conversion (ISC$n$) and least squares scale conversion (LSSC$n$), where the variable $n = 0$, 1, and 3 denotes the order of the spline.

### *B. Results*

Our first example is qualitative and uses the test image (printed text) in Fig. 2. The results of zero-order interpolation (ISC0) and least squares approximations (LSSC0) for $\Delta = 1/\sqrt{2}$ (magnification) and $\Delta = \sqrt{2}$ (reduction) are compared in Fig. 6. Clearly, the results of LSSC0 are by far superior to those obtained by nearest neighbor interpolation (ISC0). The reduced image in the latter case is unreadable. Similar comparisons for linear ($n = 1$) and cubic ($n = 3$) splines are given in Figs. 7 and 8, respectively. In all cases, LSSC results in a significant improvement for image reduction. The quality of the magnified image obtained with LSSC1 also appears to be increased; this distinction is less apparent for $n = 3$. Note that the resized images obtained using cubic splines exhibit some "ringing" near the border of the letters. This effect is best observed on the enlarged subimages (×8) shown to the right of Figs. 6–8. The ringing, which becomes more apparent with higher order splines, is similar to the Gibbs phenomenon that is usually associated with bandlimited representations (sinc interpolator). For this type of two level images, LSSC1 appears to yield images with better visual quality, probably because the oscillations near the borders of the objects are less pronounced than they are for cubic splines.

In the next series of experiments, we performed a succession of complementary image reductions and magnifications, and vice versa, using the different scale conversion techniques. The global loss of information was measured by the signal-to-noise ratio with reference to the initial image. Our test images (a) and (b) are the MRI scan shown in Fig. 1(a) and the standard "Lena" picture, respectively. The results of these experiments for image reduction are given in Table III. The LSSC outperforms ISC in all cases, although there is only marginal difference for cubic order. There is also improvement of performance of both with increasing order $n$. This observation has been confirmed by experiments with other images. In the case of an image reduction by a factor of two, we found that the results obtained with LSSC were not appreciably different from those obtained with the filtering-decimation algorithm described in [14].

$$Q(z) = \frac{(z + 4 + z^{-1})/6}{0.4886 + 0.2308[z + z^{-1}] + 0.02432[z^{2} + z^{-2}] + 0.00057[z^{3} + z^{-3}]} \tag{34}$$

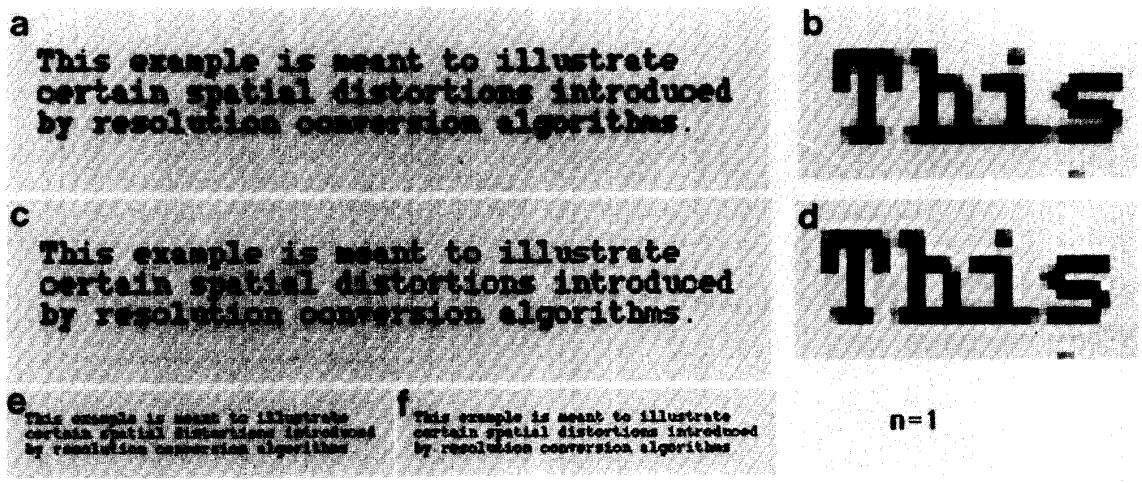


Fig. 7. Examples of image magnification and reduction using a first-order model: (a) ISC1 with $\Delta = 1/\sqrt{2}$; (b) enlarged detail of (a); (c) LSSC1 with $\Delta = 1/\sqrt{2}$; (d) enlarged detail of (c); (e) ISC1 with $\Delta = \sqrt{2}$; (f) LSSC1 with $\Delta = \sqrt{2}$.

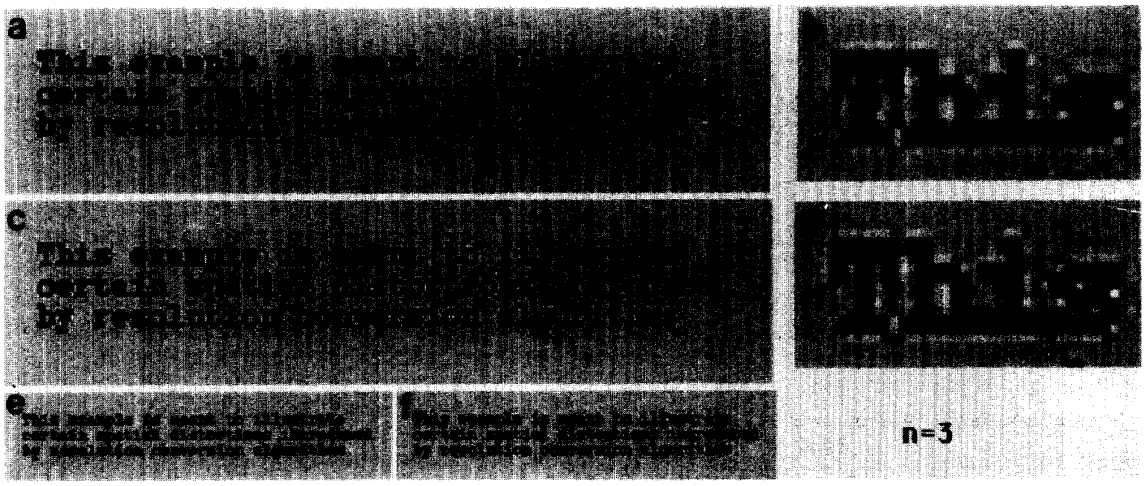


Fig. 8. Examples of image magnification and reduction using a cubic spline model: (a) ISC3 with $\Delta = 1/\sqrt{2}$; (b) LSSC3 with $\Delta = 1/\sqrt{2}$; (c) ISC3 with $\Delta = \sqrt{2}$; (d) LSSC3 with $\Delta = \sqrt{2}$.

Results for image magnification are given in Table IV. In the case of integer magnification, all methods perform ideally in the sense that the original image can be recovered exactly (within the limits of roundoff errors). In the case of a nonintegral magnification ($\sqrt{2}$), there is a loss of information that disappears gradually with higher order splines. Here again, LSSC is consistently superior (with the notable exception of $n = 0$). The high SNR value reported for ISC0 in Table IV merely expresses the fact that the initial pixel values are not lost in this approach and that perfect recovery of the original is always possible. The quantity calculated is misleading in that it fails to indicate that the visual quality of a nearest neighbor image magnification is by far the worst (c.f. Fig. 6).

### C. Discussion

i) *Advantage of least squares approximation over interpolation:* Our experimental results demonstrate the superiority of LSSC over ISC in a consistent fashion. This observation is especially true for image reduction. For some images, the differences can be quite dramatic. An example is provided by Fig. 9, which displays the approximation errors for ISC1 and LSSC1 in the case of an image reduction by $\sqrt{2}$. We have also observed experimentally that the loss of performance of ISC becomes more striking with increasing reduction factors.

ii) *Computational efficiency of the approach:* The LSSC algorithm is relatively simple to implement in practice. The resampling part of the algorithm (18) is very similar to the standard interpolation procedure. The essential difference is that the LSSC sampling function depends explicitly on the scaling parameter $\Delta$. These functions tend to have a larger support resulting in an increased number of nonzero terms in the expansion formula. The simplest approach is LSSC0, which is comparable in

Fig. 9. Comparison of the interpolative and least squares scale conversion algorithms for the MRI image in Fig. 1(a): (a) ISC1 with $\Delta = \sqrt{2}$; (b) LSSC1 with $\Delta = \sqrt{2}$; (c) approximation error for (a) (SNR = 33.65 dB); (d) approximation error for (b) (SNR = 39.25 dB).

TABLE III
COMPARISON OF IMAGE REDUCTION TECHNIQUES

| $n$ | Experimental procedure | Signal-to-Noise Ratio (a) MRI | (b) Lena |
|---|---|---|---|
| n=0 | (ISC + $\sqrt{2}$, ISC × $\sqrt{2}$) | 27.03 dB | 24.12 dB |
| | (LSSC + $\sqrt{2}$, LSSC × $\sqrt{2}$) | 32.71 dB | 28.37 dB |
| n=1 | (ISC + $\sqrt{2}$, ISC × $\sqrt{2}$) | 33.65 dB | 28.74 dB |
| | (LSSC + $\sqrt{2}$, LSSC × $\sqrt{2}$) | 39.25 dB | 31.77 dB |
| n=3 | (ISC + $\sqrt{2}$, ISC × $\sqrt{2}$) | 42.02 dB | 32.30 dB |
| | (LSSC + $\sqrt{2}$, LSSC × $\sqrt{2}$) | 42.61 dB | 32.53 dB |
| n=0 | (ISC + 2, ISC × 2) | 24.74 dB | 21.74 dB |
| | (LSSC + 2, LSSC × 2) | 29.50 dB | 25.66 dB |
| n=1 | (ISC + 2, ISC × 2) | 31.56 dB | 26.45 dB |
| | (LSSC + 2, LSSC × 2) | 32.62 dB | 27.19 dB |
| n=3 | (ISC + 2, ISC × 2) | 35.35 dB | 26.80 dB |
| | (LSSC + 2, LSSC × 2) | 36.13 dB | 27.88 dB |

TABLE IV
QUALITATIVE ASSESSMENT OF IMAGE MAGNIFICATION TECHNIQUES

| $n$ | Experimental procedure | Signal-to-Noise Ratio (a) MRI | (b) Lena |
|---|---|---|---|
| n=0 | (ISC × $\sqrt{2}$, ISC + $\sqrt{2}$) | >60 dB | >60 dB |
| | (LSSC × $\sqrt{2}$, LSSC + $\sqrt{2}$) | 38.20 dB | 33.68 dB |
| n=1 | (ISC × $\sqrt{2}$, ISC + $\sqrt{2}$) | 39.45 dB | 34.08 dB |
| | (LSSC × $\sqrt{2}$, LSSC + $\sqrt{2}$) | 57.35 dB | 50.98 dB |
| n=3 | (ISC × $\sqrt{2}$, ISC + $\sqrt{2}$) | 59.09 dB | 50.67 dB |
| | (LSSC × $\sqrt{2}$, LSSC + $\sqrt{2}$) | >60 dB | >60 dB |
| n=0 | (ISC × 2, ISC + 2) | >60 dB | >60 dB |
| | (LSSC × 2, LSSC+ 2) | >60 dB | >60 dB |
| n=1 | (ISC × 2, ISC + 2) | >60 dB | >60 dB |
| | (LSSC × 2, LSSC+ 2) | >60 dB | >60 dB |
| n=3 | (ISC × 2, ISC + 2) | >60 dB | >60 dB |
| | (LSSC × 2, LSSC+ 2) | >60 dB | >60 dB |

complexity to a standard bilinear interpolation (ISC1). For higher order splines, LSSC also requires the use of a postfilter absent in ISC.

We used two basic strategies to improve the computational efficiency of these algorithms. The first was to take advantage of the separability property and to process the rows and columns of an image successively using one-dimensional operators. The second was to implement all digital filters recursively by decomposing them into a cascade of simple exponential causal and anti-causal operators. On our low-end workstation (standard Macintosh II fx), the CPU time for reducing the 238× 253

MRI scan by a factor of $\sqrt{2}$ was of the order of 1 s for ISC0, 10 s for LSSC0, 8 s for ISC1 (c.f. Fig. 9(a)), 27 s for LSSC1 (c.f. Fig. 9(b)), 19 s for ISC3, and 39 s for LSSC3.

iii) *Link with the digital-filter based decimation-expansion techniques:* As shown in the Appendix, the present approach for $\Delta = m$ is equivalent to the filtering-decimation procedure described in [14]. Specifically, we have that

$$s_m(k) = \left[\overset{\circ}{h}{}_m^n * s_1\right]_{\downarrow m}(k) \tag{35}$$

where $[\cdot]_{\downarrow m}$ denotes the down-sampling by a factor of $m$, and where the prefilter $\overset{\circ}{h}{}_m^n$ is characterized by its transfer function

$$\overset{\circ}{h}{}_m^n(k) \overset{z}{\longleftrightarrow} \overset{\circ}{H}{}_m^n(z) = \frac{1}{m}\frac{B_1^n(z^m)B_1^{2n+1}(z)U_m^n(z)}{B_1^{2n+1}(z^m)B_1^n(z)}. \tag{36}$$

$B_1^n(z)$ is the $z$-transform of a discrete $B$-spline of order $n$ (c.f. (4)) and $U_m^n(z)$ is defined by

$$u_m^n(k) \overset{z}{\longleftrightarrow} U_m^n(z) = \frac{z^{k_0}}{m^n}\left(\sum_{k=0}^{m-1} z^{-k}\right)^{n+1} \tag{37}$$

with $k_0 = (n+1)(m-1)/2$. Note that a similar filtering-decimation procedure can also be derived by minimizing the discrete $l_2$-norm [12], [13], but the prefilters are no longer the same.

Another case of interest is a signal magnification by an integer factor $m(\Delta = 1/m)$. For this special situation, it can be shown that $S_{1/m}^n \supset S_1^n$, provided that $n$ and $m$ are not both even. It follows that the initial polynomial spline representation of our signal $s_1(x)$ is already included in the finer resolution space $S_{1/m}^n$. Hence, it should be possible to obtain the sample values $s_m(k)$ of the expanded signal by simple interpolation, which suggests that the ISC and LSSC algorithms are equivalent for $\Delta = 1/m$. In the appendix, we prove that this is indeed the case. Specifically, we show that the algorithm described in Section III-B is equivalent to the following procedure

$$s_{1/m}(k) = h_m^n * [s_1]_{\uparrow m}(k) \tag{38}$$

where $h_m^n$ is the impulse response of a polynomial spline interpolator with a zooming factor $m$, and where $[\cdot]_{\uparrow m}$ denotes the up-sampling by a factor of $m$. Equation (38) is precisely the digital filtering formulation of the ISC algorithm for $\Delta = 1/m$ initially proposed in [8]. The transfer function of the corresponding spline interpolator is

$$h_m^n(k) \overset{z}{\longleftrightarrow} H_m^n(z) = \frac{B_1^n(z)U_m^n(z)}{B_1^n(z^m)}. \tag{39}$$

Note that the digital filters $h_m^n$ and $\overset{\circ}{h}{}_m^n$ satisfy the discrete biorthogonality condition

$$\left[h_m^n * \overset{\circ}{h}{}_m^n\right]_{\downarrow m}(k) = \delta_k \tag{40}$$

These results imply that an image magnification followed by a reduction by the same integer factor $m$ should leave the original signal unchanged. This fact has been observed experimentally for both algorithms (c.f. lower half of Table IV). This property obviously does not apply for noninteger magnification factors, unless the order of the spline is sufficiently large.

iv) *Link with Shannon sampling theory:* There is a close relationship between the present approach and the optimal procedure dictated by Shannon's sampling theory. In fact, this latter approach corresponds to the limiting case $n \to +\infty$ [7], [15]. The classical formulation is attractive conceptually because it uses a simple bandlimited representation of signals. However, the direct resampling algorithm is difficult to implement in practice because of the slow decay of $\mathrm{sinc}(x)$ (the impulse response of the ideal lowpass filter). Fortunately, we have seen that there is an alternative FFT-based algorithm that is applicable for certain rational scaling factors $\Delta$ [22].

We note that Shannon's sampling theory treats signal magnification and reduction differently. First, there is no loss of information associated with signal magnification, which implies that the process is fully reversible. Moreover, the use of a prefilter is not necessary because the coarser level signal is already bandlimited. These observations are in agreement with our experimental findings: i) the performance of our algorithm for signal magnification improves with higher order splines, and ii) the distinction between the ISC and LSSC is less and less significant for higher order splines (c.f. Table IV).

The classical approach for signal reduction is to bandlimit the signal with an ideal lowpass filter prior resampling. This prefiltering step is important because it suppresses aliasing errors. The LSSC algorithm uses a similar procedure—a prefilter designed to minimize the approximation error. The ISC algorithm with no such built-in mechanism exhibits poorer performance for signal reduction.

v) *Other potential approaches:* This work has focused almost exclusively on spline representations of signals, mainly because of their simplicity of implementation. In principle, similar least squares methods could be derived for more general functional representations, for example, the class of Hilbert spaces considered in [25] and [26]. Kida and Mochizuki also present a very general form of interpolation that depends on the sampling model and is optimal in a well-defined sense [27]. Finally, Peleg *et al.* have proposed an original approach for trading spatial for gray-level resolution and vice versa [28]. Unfortunately, it requires a lengthy linear programming

optimization on a pixel-by-pixel basis and is therefore difficult to apply in practice.

## VI. Conclusion

In this paper, we have described a new family of techniques for resizing digital images. Our design principle is to fit images by continuous spline models and to implement the transformation that minimizes the error between the original image and its rescaled version. This approach (LSSC) appears to be better than standard interpolation methods in the sense that the rescaled image is a more faithful copy of the original, including lesser visual distortions and improved suppression of aliasing artifacts. The same algorithm works for any (non-integer) scaling factor $\Delta \geq 0$; it is equally valid for signal magnification and reduction.

We have emphasized both the practical and theoretical aspects of these techniques. In particular, we have studied the various steps of the implementation of LSSC and have proposed fast computational solutions. We have also brought out links with a number of earlier techniques. For instance, we have shown the equivalence between the present approach and earlier digital filter based expansion-decimation techniques in the particular case of a signal expansion or reduction by an integer factor. We have also discussed the asymptotic convergence of LSSC to the classical procedure dictated by Shannon's sampling theorem. Based on our previous error estimates, the cubic spline algorithm (LSSC3) can be considered as a good approximation of this limiting case (bandlimited signal approximation) [7], [15]. For the examples tested, this technique led to the smaller approximation error, but had the tendency to introduce oscillations (Gibbs phenomenon). The first order spline algorithm (LSSC1) was found to provide a good compromise between performance and an attenuation of these oscillations; it may therefore be preferred for certain applications.

## Appendix
## Integer Scale Conversion

In this appendix, we consider the special cases of signal reduction and magnification by an integer factor $m$. In particular, we establish the connection between the LSSC algorithm and a number of earlier techniques [8], [14]. These results are valid provided that $m$ and $n$ are not both even.

### A. Reduction by a Factor of $m$

We first recall that the expanded $B$-spline can be represented by the following expansion [14]

$$\beta_m^n(x) = \sum_{k=-\infty}^{+\infty} u_m^n(k)\beta^n(x-k) \tag{A.1}$$

where the sequence $u_m^n$ is defined by (37). By using the property that $\beta^n * \beta^n(x) = \beta^{2n+1}(x)$ (c.f. (1)), it is not difficult to show that the sampling function defined by (19) is simply

$$\xi_m^n(x) = \frac{1}{m}\sum_{k=-\infty}^{+\infty} u_m^n(k)\beta^{2n+1}(x-k). \tag{A.2}$$

By resampling this function at multiples of $m$ and using (18), we get the expression for the dual spline coefficients

$$d_m(k) = \frac{1}{m}\left[b^{2n+1} * u_m^n * c_1\right]_{\downarrow m}(k)$$

where $[\cdot]_{\downarrow m}$ denotes the down-sampling by a factor of $m$. To get a direct relation between the sample values $s_1$ and $s_m$ (cardinal representation), we perform the appropriate changes of coordinate system

$$s_m(k) = \frac{1}{m}(b^{2n+1})^{-1} * b^n \times \left[(b^n)^{-1} * b^{2n+1} * u_m^n * s_1\right]_{\downarrow m}(k). \tag{A.3}$$

Note that this expression is fully compatible with the results from Theorem 2 in [14]. It can be further manipulated to yield

$$s_m(k) = \frac{1}{m}\left[\left[(b^{2n+1})^{-1} * b^n\right]_{\uparrow m} * (b^n)^{-1} * b^{2n+1} * u_m^n * s_1\right]_{\downarrow m}(k) \tag{A.4}$$

where the operator $[\cdot]_{\uparrow m}$ denotes the up-sampling by a factor of $m$. The optimal prefilter $\overset{\circ}{h}{}_m^n$ in (36) is finally obtained by regrouping all convolution operators that act on the signal $s_1$.

### B. Magnification by a Factor of $m$

We now consider the case $\Delta = 1/m$. By performing the change of variable $y = x/m$ in (19) and (A.2), it is not difficult to show that

$$\xi_{1/m}^n(y) = \sum_{k=-\infty}^{+\infty} u_m^n(k)\beta_{1/m}^{2n+1}(y - k/m). \tag{A.5}$$

We then substitute this expression in (18), which yields

$$d_{1/m}(k) = u_m^n * b^{2n+1} * [c_1]_{\uparrow m}(k).$$

Finally, we express the coefficients in this equation in terms of the sample values $s_1$ and $s_{1/m}$ (c.f. (8) and (22)) and make the following manipulation:

$$\begin{aligned} s_{1/m}(k) &= b^n * (b^{2n+1})^{-1} * u_m^n * b^{2n+1} * \left[(b^n)^{-1} * s_1\right]_{\uparrow m}(k) \\ &= b^n * u_m^n * \left[(b^n)^{-1}\right]_{\uparrow m} * [s_1]_{\uparrow m}(k). \end{aligned} \tag{A.6}$$

This result, which is equivalent to (38) and (39), is precisely the polynomial spline interpolation algorithm described in [8].

## References


[1] W. K. Pratt, *Digital Image Processing*. New York: Wiley, 1978.

[2] J. A. Parker, R. V. Kenyon, and D. E. Troxel, "Comparison of interpolating methods for image resampling," *IEEE Trans. Med. Imag.*, vol. MI-2, pp. 31–39, 1983.

[3] R. Bernstein and G. C. Stierhoff, "Precision processing of earth image data," *Amer. Scientist*, vol. 64, pp. 500–508, Sept.–Oct. 1976.

[4] R. G. Keys, "Cubic convolution interpolation for digital image processing," *IEEE Trans. Acoust., Speech, Signal Processing*, vol. ASSP-29, pp. 1153–1160, 1981.

[5] S. K. Park and R. A. Showengerdt, "Image reconstruction by parametric convolution," *Comput. Vision, Graphics, Image Processing*, vol. 20, pp. 258–272, Sept. 1983.
[6] H. S. Hou and H. C. Andrews, "Cubic splines for image interpolation and digital filtering," *IEEE Trans. Acoust., Speech, Signal Processing*, vol. ASSP-26, pp. 508–517, 1978.
[7] A. Aldroubi, M. Unser, and M. Eden, "Cardinal spline filters: stability and convergence to the ideal sinc interpolator," *Signal Processing*, vol. 28, pp. 127–138, Aug. 1992.
[8] M. Unser, A. Aldroubi. and M. Eden, "Fast $B$-spline transforms for continuous image representation and interpolation," *IEEE Trans. Pattern Anal. Machine Intell.*, vol. 13, pp. 277–285, Mar. 1991.
[9] R. E. Crochiere and L. R. Rabiner, "Interpolation and decimation of digital signals," *Proc. IEEE*, vol. 69, pp. 300–331, Mar. 1981.
[10] ——, *Multirate Digital Signal Processing*. Englewood Cliffs, NJ: Prentice-Hall, 1983.
[11] J. G. Proakis and D. G. Manolakis, *Introduction to Digital Signal Processing*. New York: Macmillan, 1990.
[12] R. Hummel, "Sampling for spline reconstruction," *SIAM J. Appl. Math.*, vol. 43, pp. 278–288, 1983.
[13] A. Aldroubi, M. Unser, and M. Eden, "Discrete spline filters for multiresolutions and wavelets of $l_2$," *SIAM J. Math. Anal.*, vol. 25, pp. 1412–1432, Sept. 1994.
[14] M. Unser, A. Aldroubi, and M. Eden, "The $L_2$ polynomial spline pyramid," *IEEE Trans. Pattern Anal. Mach. Intell.*, vol. 15, pp. 364–379, Apr. 1993.
[15] ——, "Polynomial spline signal approximations: filter design and asymptotic equivalence with Shannon's sampling theorem," *IEEE Trans. Inform. Theory*, vol. 38, pp. 95–103, Jan. 1992.
[16] I. J. Schoenberg, "Contribution to the problem of approximation of equidistant data by analytic functions," *Quart. Appl. Math.*, vol. 4, pp. 45–99, 112–141, 1946.
[17] ——, "Cardinal interpolation and spline functions," *J. Approximation Theory*, vol. 2, pp. 167–206, 1969.
[18] C. de Boor, *A Practical Guide to Splines*. New York: Springer-Verlag, 1978.
[19] P. M. Prenter, *Splines and Variational Methods*. New York: Wiley, 1975.
[20] C. E. Shannon, "Communication in the presence of noise," *Proc. I.R.E.*, vol. 37, pp. 10–21, Jan. 1971.
[21] W. Feller, *An Introduction to Probability Theory and its Application*. New York: Wiley, 1971, vol. II.
[22] D. Fraser, "Interpolation by the FFT revisited—An experimental evaluation," *IEEE Trans. Acoust., Speech, Signal Processing*, vol. 37, pp. 665–675, May 1989.
[23] T. J. Cavicchi, "DFT time-domain interpolation," *Proc. Inst. Elec. Eng.-F*, vol. 139, pp. 207–211, 1992.
[24] M. Unser, A. Aldroubi, and M. Eden, "$B$-spline signal processing. Part II: Efficient design and applications," *IEEE Trans. Signal Processing*, vol. 41, pp. 834–848, Feb. 1993.
[25] A. Aldroubi and M. Unser, "Sampling procedures in function spaces and asymptotic equivalence with Shannon's sampling theory," *Numer. Funct. Anal. Optimiz.*, vol. 15, pp. 1–21, Feb. 1994.
[26] H. Ogawa, "A generalized sampling theorem," *Electron. Commun. Japan*, Part 3, vol. 72, pp. 97–105, Mar. 1989.
[27] T. Kida and H. Mochizuki, "Generalized interpolatory approximation of multidimensional signals having the minimum measure of error," *IEICE Trans. Fundamentals*, vol. E74-A, pp. 794–805, July 1992.
[28] S. Peleg, M. Werman, and H. Rom, "A unified approach to the change of resolution: space and gray-level," *IEEE Trans. Pattern Anal. Machine Intell.*, vol. 11, pp. 739–742, July 1989.

**Michael Unser** (M'88–SM'94) was born in Zug, Switzerland, on April 9, 1958. He received the M.S. (with highest honors) and Ph.D. degrees in electrical engineering in 1981 and 1984, respectively, from the Swiss Federal Institute of Technology, Lausanne, Switzerland.

He is currently a Visiting Scientist with the Biomedical Engineering and Instrumentation Program, National Institutes of Health, Bethesda, which he joined in 1985. He has also been affiliated with INSERM (French National Institutes of Health and Biomedical Research) since 1988. His research interests include the application of image processing and pattern recognition techniques to various biomedical problems, multiresolution algorithms, wavelet transforms, and the use of splines in signal processing.

Dr. Unser was awarded the Brown–Bovery Prize in 1984 for his work on texture analysis and automated inspection. He is the author or coauthor of more than 50 papers in professional journals. He serves as an Associate Editor for the IEEE TRANSACTIONS ON IMAGE PROCESSING and the IEEE SIGNAL PROCESSING LETTERS. He is also a member of the Multidimensional Signal Processing Committee of the IEEE Signal Processing Society and is on the editorial board of *Signal Processing*.

**Akram Aldroubi** received the M.S. in electrical engineering in 1982 from l'Ecole Polytechnique Federale de Lausanne, Switerland, where he was awarded the Rene Cousin Prize for excellence. He received the M.S. and the Ph.D. in Mathematics in 1984 and 1987, respectively, from Carnegie–Mellon University, Pittsburgh, PA.

He is currently a Senior Staff Fellow at the Biomedical Engineering and Instrumentation Program, National Institutes of Health. His research interests include functional analysis, partial differential equations, and signal/image processing.

Dr. Aldroubi is a member of the American Mathematical Society.

**Murray Eden** (M'60–F'73–LF'91) was born in Brooklyn, New York, on August 17, 1920. He received the B.S. degree from City College of New York in 1939 and a Ph.D. from the University of Maryland in 1951.

He is Scientist Emeritus and former director of the Biomedical Engineering and Instrumentation Program, National Center for Research Resources, National Institutes of Health, and Professor of Electrical Engineering, Emeritus, Massachusetts Institute of Technology. His research interests include pattern recognition, analytical uses of image processing, and models for perception.